

# 近熱外中性子の利用

山形大学 理学部

亀田恭男

RCNP研究会 研究用原子炉を用いた原子核素粒子物理学  
2022年5月30日(月)～31日(火)  
大阪大学核物理研究センター、zoomによるハイブリッド開催

## 液体、非晶質物質の構造解析

### 【中性子回折実験の優位性】

軽元素の構造を精度良く求められる。

同位体置換試料の実験データ

→ 部分構造因子、部分分布関数の導出が実験から直接可能。

→ 注目するイオンの溶媒和構造、溶媒分子間水素結合構造

### 【定常炉による実験の優位性】

[定常炉]

Hを多量に含む試料の非弾性散乱補正が比較的容易に行える。

試料の非弾性散乱効果を含む散乱断面積 → **Qの多項式で近似可能**

[パルス中性子]

Hを多量に含む試料の非弾性散乱補正が非常に困難。

$^0\text{H}_2\text{O}$ のself散乱区強度を用いた補正方法 → **水溶液以外ではあまりうまくいかない**

## 【液体、非晶質物質の構造解析のために重要な要件】

- ・統計精度が良い(数時間の測定で、1点当たり>数10万~数100万カウント)
- ・良好な安定性 (線源、検出システム: 数時間で揺らぎは <0.1%)
- ・できる限り広い $Q (= 4\pi/\lambda \cdot \sin\theta)$ 範囲のデータを取得可能(できれば $Q > 20 \text{ \AA}^{-1}$ )

実空間の分解能 $\Delta r = 3.791/Q_{\max}$  (Wright & Leadbetter, *Phys. Chem. Glass.* **1976**, 17, 122-145.)

$$Q_{\max} = 10 \text{ \AA}^{-1} \rightarrow \Delta r = 0.38 \text{ \AA}, Q_{\max} = 20 \text{ \AA}^{-1} \rightarrow \Delta r = 0.19 \text{ \AA}$$

- ・広い試料スペース(高温炉等が設置可能)

## 【中性子源に求められる性能】

- ・波長: 0.5  $\text{\AA}$  ( $2\theta = 120^\circ$  で  $Q = 21.8 \text{ \AA}^{-1}$ )

$$0.7 \text{ \AA} \text{ (} 2\theta = 120^\circ \text{ で } Q = 15.5 \text{ \AA}^{-1}\text{)}$$

ホットソースが必要

## 【検出器に求められる性能】

- ・できる限り高い検出効率

PSD, 試料を取り囲むように多数の検出器を並べる配置

## 【現在稼働中の液体、非晶質構造解析装置】

ラウエ・ランジュバン研究所(フランス)

HFR炉(1993年改造) 出力 58MW

・D4c回折計 ( $\lambda = 0.35, 0.5, 0.7 \text{ \AA}$ ) ( $2\theta = 1.5-140^\circ$  )

大強度粉末回折計

$0.5 < Q < 33.7 \text{ \AA}^{-1}$  ( $\lambda = 0.35 \text{ \AA}$ )

$0.3 < Q < 23.6 \text{ \AA}^{-1}$  ( $\lambda = 0.5 \text{ \AA}$ )

$0.2 < Q < 16.9 \text{ \AA}^{-1}$  ( $\lambda = 0.7 \text{ \AA}$ )

・D20回折計 ( $\lambda = 0.82, 0.88, 0.94, 1.07 \text{ \AA}$ ) ( $2\theta = 1.5-153.6^\circ$  )

大強度粉末回折計

・D3回折計 ( $\lambda = 0.42 - 0.843 \text{ \AA}$ )

偏極中性子散乱実験

レオン・ブリリュアン研究所(フランス)

ORPHEE炉(1980年) 出力 15 MW

・7C2回折計 ( $\lambda = 0.58, 0.7, 1.11 \text{ \AA}$ )

Q-range:  $0.3 < Q < 20 \text{ \AA}^{-1}$

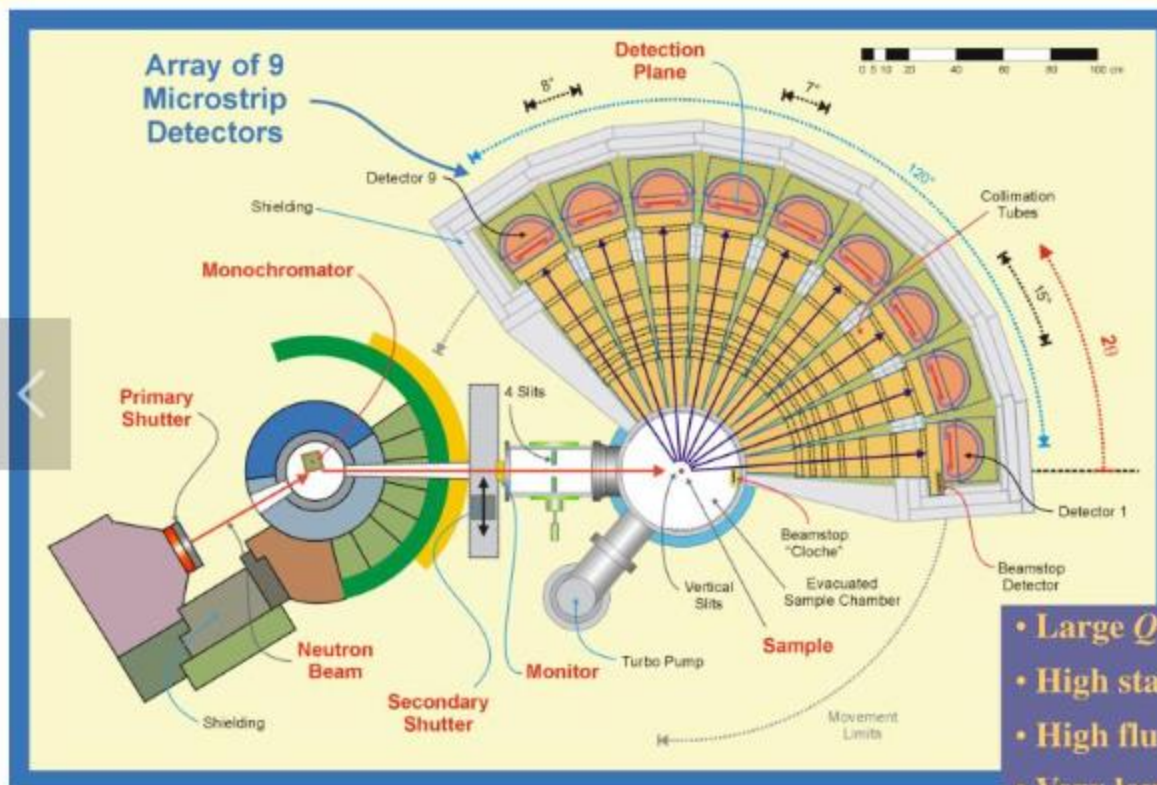
日本原子力研究開発機構(日本)

JRR-3炉(1990年) 出力 20 MW

・4G (GPTAS)分光器 ( $\lambda = 1.1 \text{ \AA}$ ) ( $2\theta = 0 - 120^\circ$  )

Q-range:  $0.3 < Q < 10 \text{ \AA}^{-1}$

# D4C (ILL)



- Large  $Q$ -range
- High stability
- High flux
- Very low background
- Simpler corrections

D4C diffractometer ( $\lambda = 0.5 \text{ \AA}$ )  $^{18}\text{O}/^{\text{nat}}\text{O}$  Isotopic Substitution Experiments  
 A. Zeidler, P. S. Salmon, H. Fisher, J. C. Neuefeind, J. M. Simonson, T. E. Markland,  
*J. Phys. Condens. Matter*, **2012**, 24, 284126.

$$b_{\text{natO}} = 0.5803 \times 10^{-12} \text{ cm}, b_{^{18}\text{O}} = 0.6009 \times 10^{-12} \text{ cm}$$

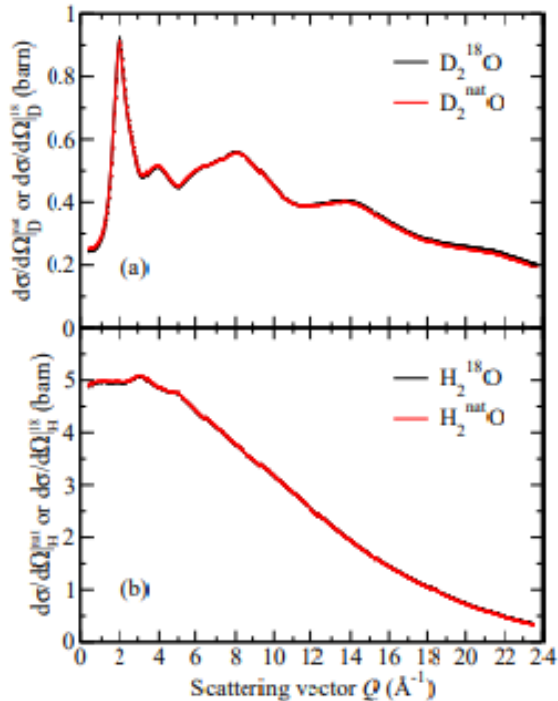


**Figure 2.** The differential scattering cross sections,  $d\sigma/d\Omega$ , as obtained from the diffraction patterns measured for samples of (a)  $\text{D}_2^{\text{nat}}\text{O}$  and  $\text{D}_2^{18}\text{O}$  or (b)  $\text{H}_2^{\text{nat}}\text{O}$  and  $\text{H}_2^{18}\text{O}$ . The error bars are much smaller than the thickness of a line. The slope on each data set arises from inelasticity effects and is more pronounced the lighter the nuclei.

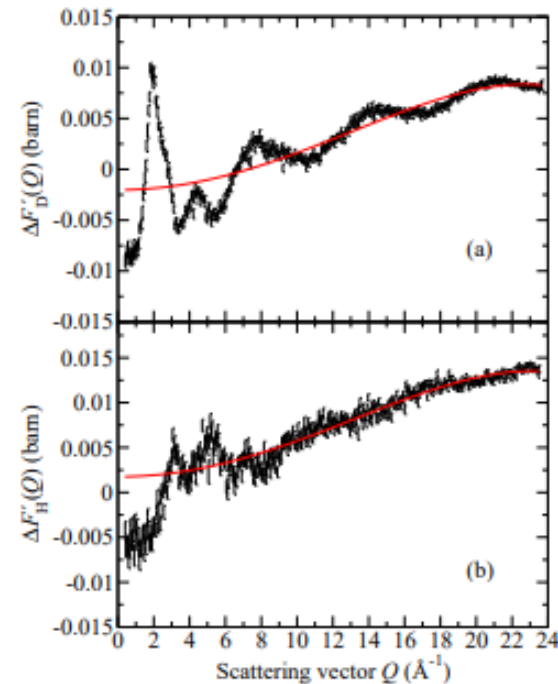


**Figure 3.** The first difference functions (a)  $\Delta F'_D(Q)$  and (b)  $\Delta F'_H(Q)$  before the application of a correction for residual inelasticity effects. The vertical bars give the statistical errors on the data points and the solid (red) curves give the fitted residual inelasticity corrections  $\Delta P_D(Q)$  and  $\Delta P_H(Q)$ .

D4C diffractometer ( $\lambda = 0.5 \text{ \AA}$ ) 4 m aqueous  $^{\text{nat}}\text{KCl}$  and  $^{41}\text{KCl}$  solutions.

P. E. Mason, L. Tavagnacco, M. –L. Saboungi, T. Hansen, H. E. Fischer, G. W. Neilson, T. Ichiye, J. W. Brady  
*J. Phys. Chem. B*, **2019**, *123*, 10807-10813.

$$b_{\text{natK}} = 0.367 \times 10^{-12} \text{ cm}, b_{^{41}\text{K}} = 0.269 \times 10^{-12} \text{ cm}$$

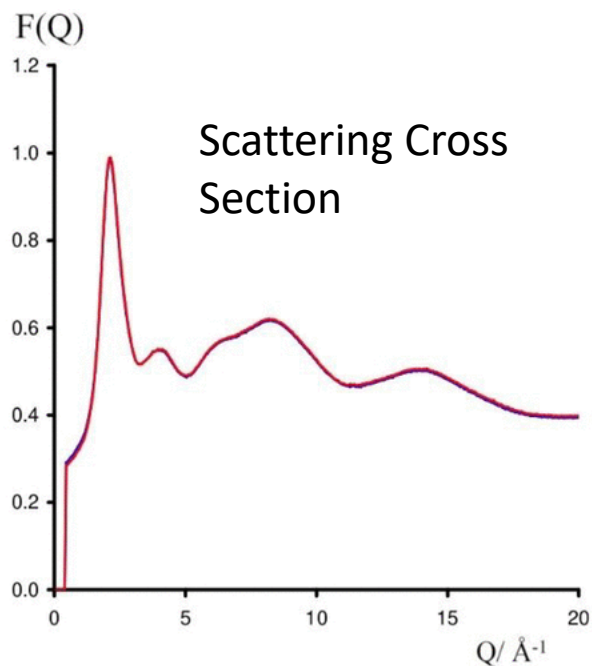


Figure 1. Total neutron scattering patterns of 4 m KCl (red) and  $^{41}\text{KCl}$  (blue) in  $\text{D}_2\text{O}$ .

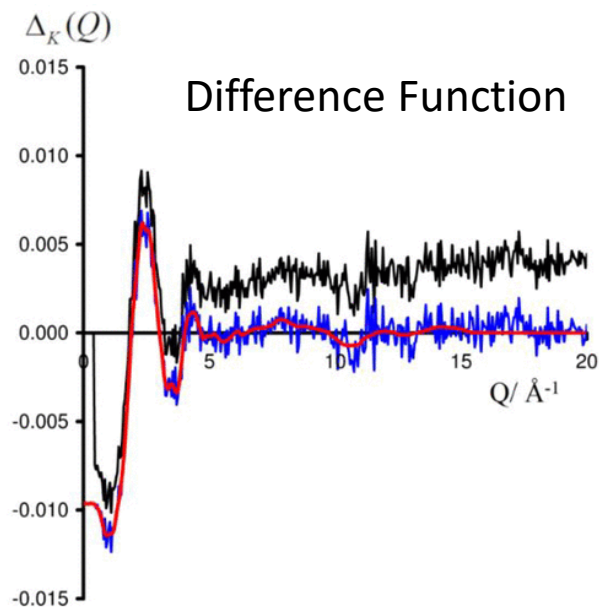
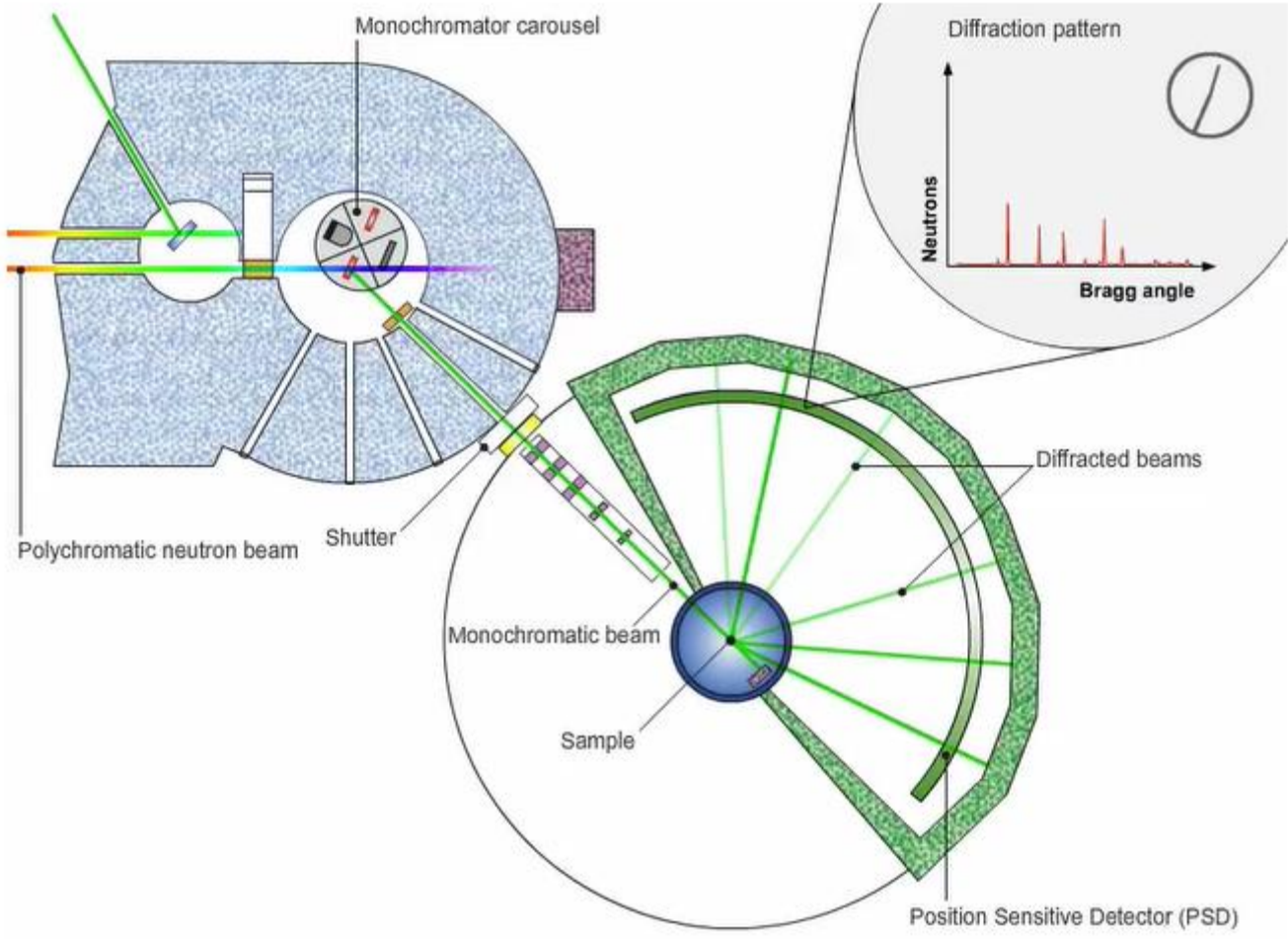


Figure 2. Raw first order difference function  $\Delta_{\kappa}(Q)$  (black), the function after a background correction (blue) consisting of the subtraction of a gradient to ensure that the function has a mean of 0 and asymptotically approaches 0, and the spline used for subsequent analysis in this paper (red). (34) The justification for this subtraction is shown in a video in the [Supporting Information](#).

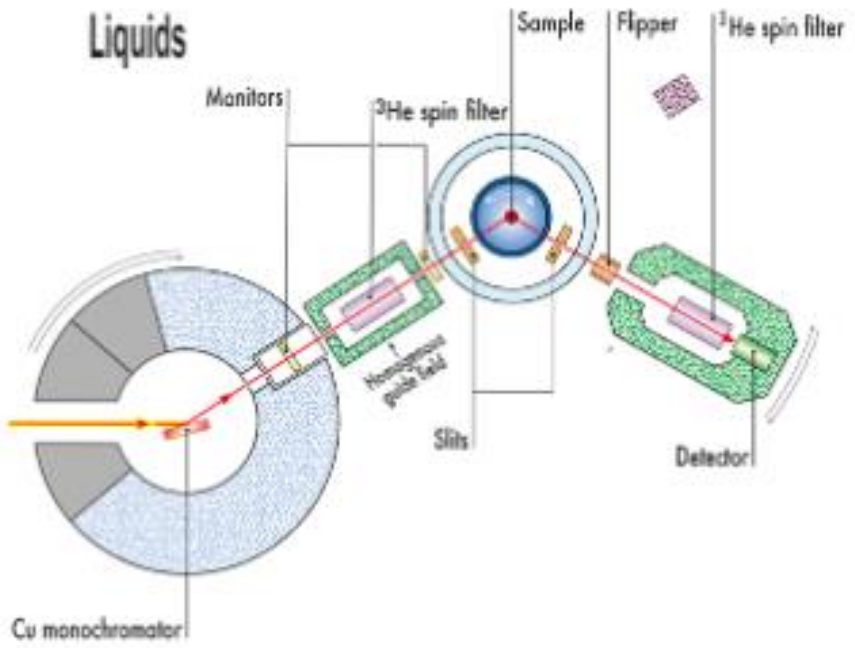


# D20 diffractometer (ILL)





# D3 diffractometer (ILL)



D3 diffractometer ILL,  $\lambda = 0.5 \text{ \AA}$

“Liquid Water”

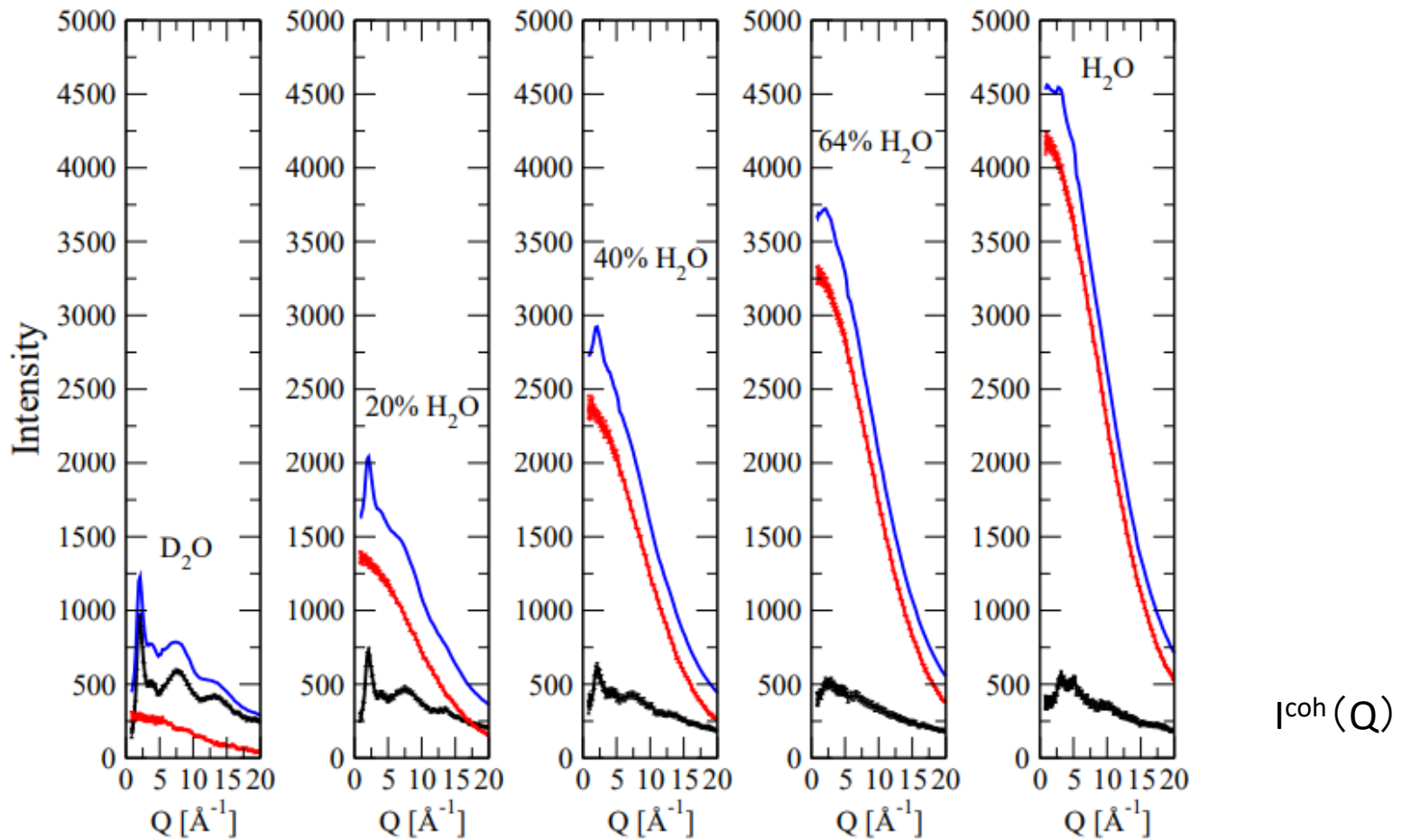
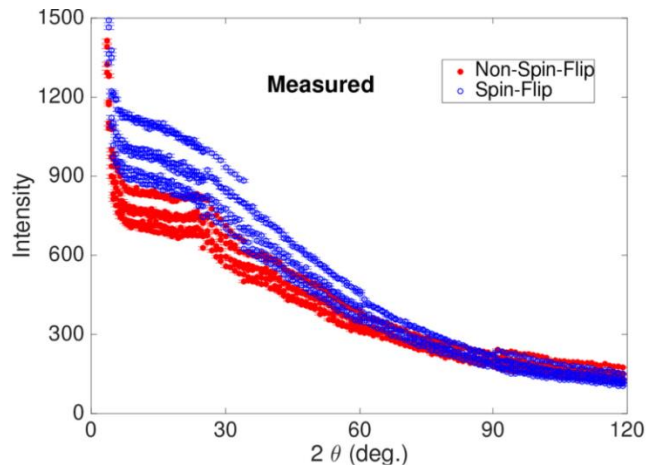


FIG. 4: Measured spin-incoherent (red lines) and coherent (black lines) intensities for 5 mixtures of light and heavy water. Light water content (from left to right): 0, 20, 40, 64 and 100 %. Blue lines: sums of the (here, separately measured) coherent and incoherent intensities, which therefore represent the neutron diffraction signal measurable without polarization analysis. If one wishes to reach the coherent intensities (black curves) from non-polarised data then a large number must be approximated (individual points of the red curves) and subtracted from another large number (individual points of the blue curves) and the desired result is a small number (individual points of the black curves). That is, taking the standard (non-polarised) way, the statistical errors only are large enough to render the entire analysis problematic, not to mention systematic uncertainties in conjunction with estimating the (spin-)incoherent contributions.

## D3 diffractometer



## D7 diffractometer

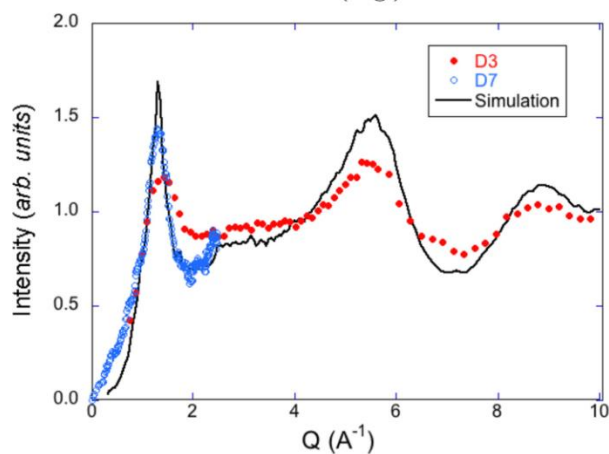
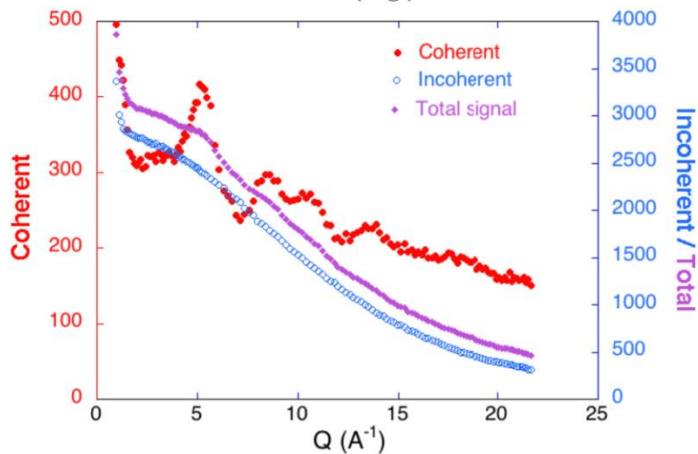
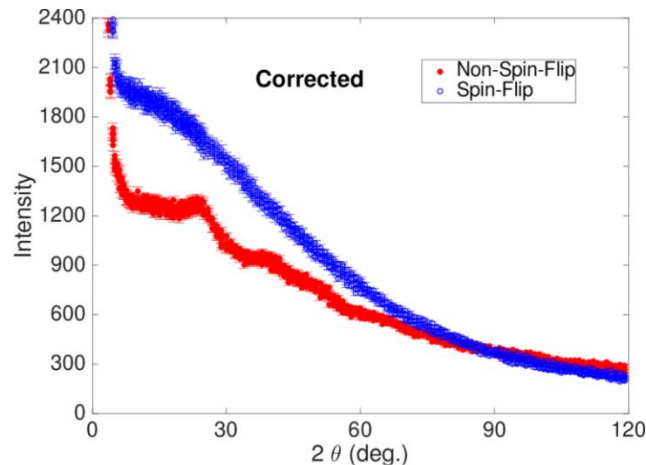
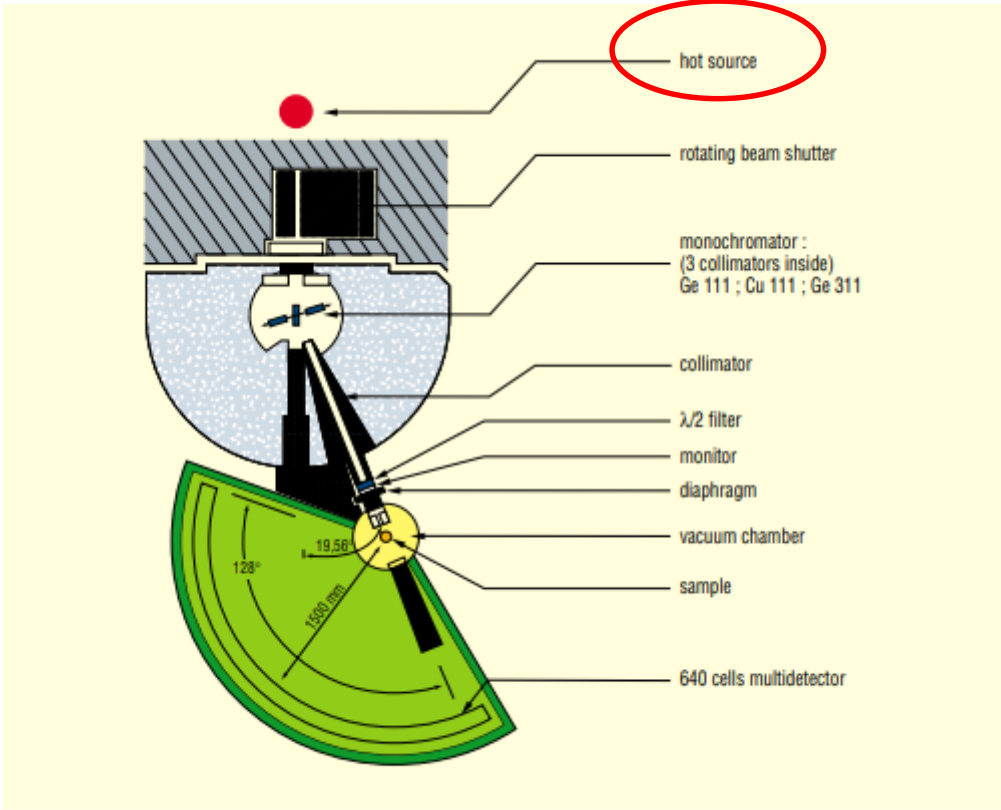


Fig. 5. Data reduction in the case of Lactulose at room temperature. Top left and right: measured and corrected intensities, respectively. Bottom left: coherent, incoherent and total signals. Note the expanded (left hand side) scale for the coherent intensities. Bottom right: comparison to a measurement of the same sample on the D7 [diffractometer](#) of the ILL. The data have not been corrected for instrument resolution, hence the different peak widths.

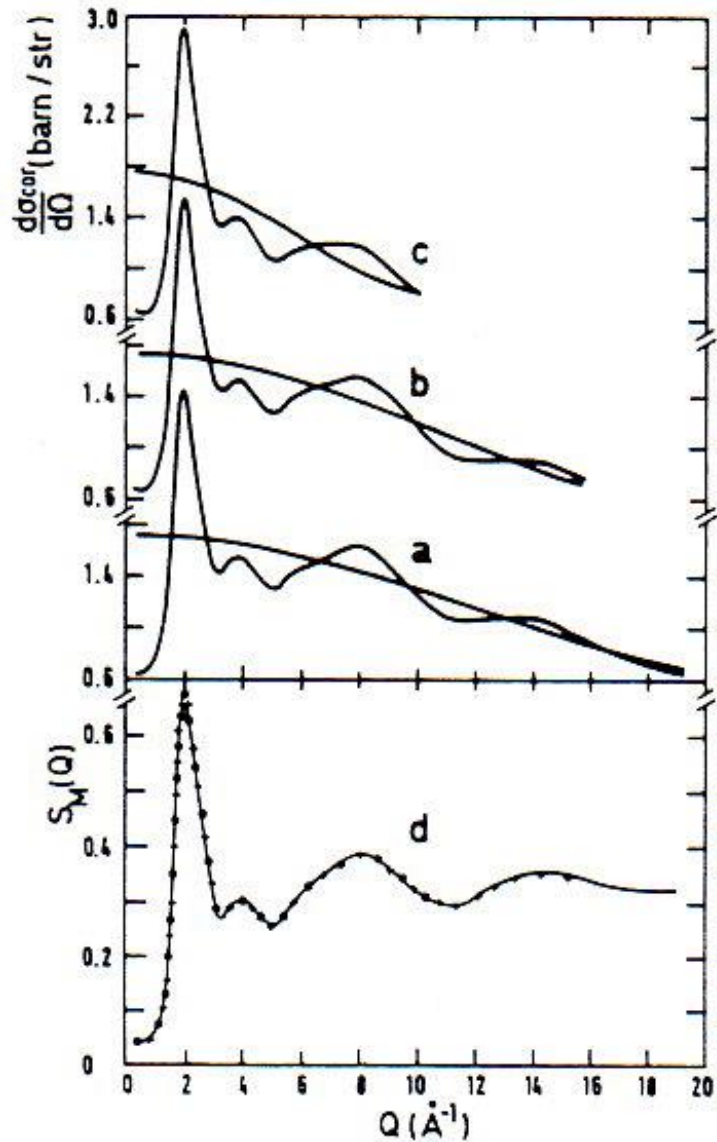
# 7C2 diffractometer



*General layout of the diffractometer 7 C2.*

Liquid D<sub>2</sub>O, 7C2 diffractometer

M. -C. Bellissent-Funel, L. Bosio, J. Teixeira, *J. Phys.: Condens. Matter*, **1991**, 3, 4065-4074.



$\lambda = 1.116 \text{ \AA}$

$\lambda = 0.712 \text{ \AA}$

$\lambda = 0.587 \text{ \AA}$

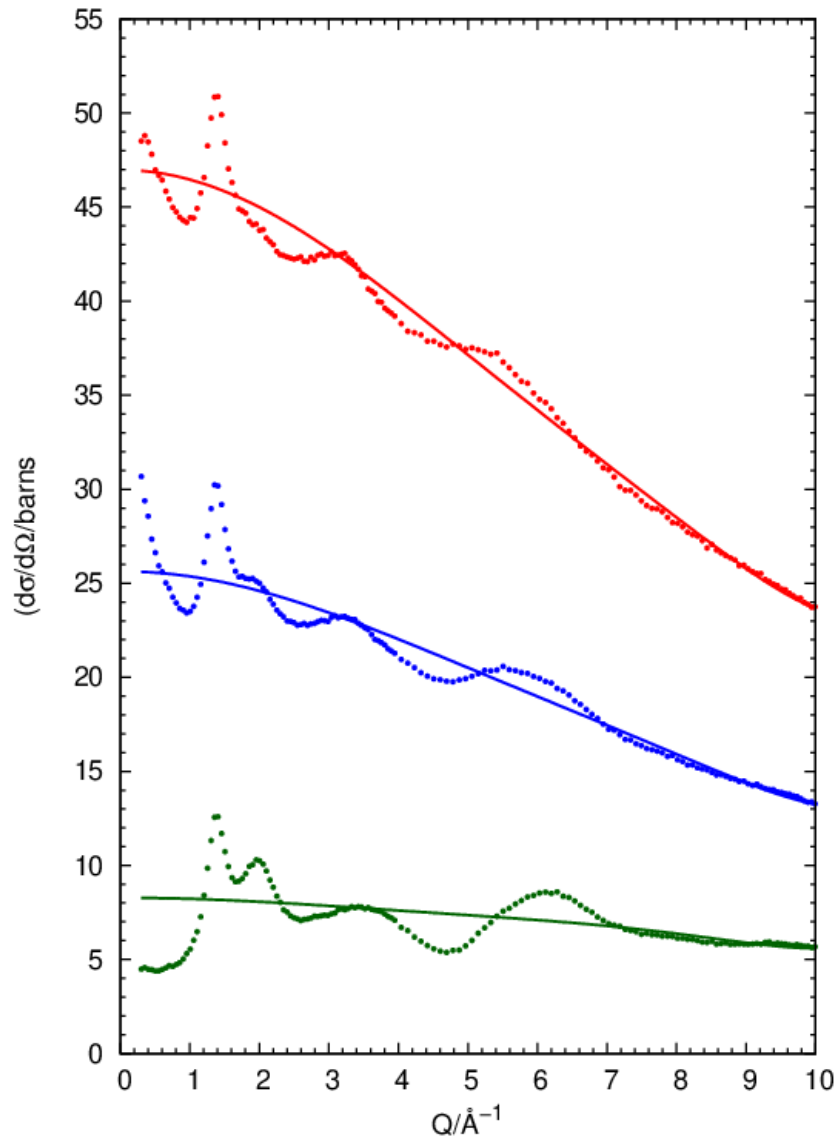


## 4G diffractometer installed at JRR-3M reactor



# Liquid benzene

$C_6X_6$  (X: D,  $^0H$ ,  $^{02}H$ ) JRR-3M 4G spectrometer, 2021.10.11-13



JRR-3M  
4G diffractometer  
 $\lambda = 1.089 \text{\AA}$

H:D = 64:36  
11h

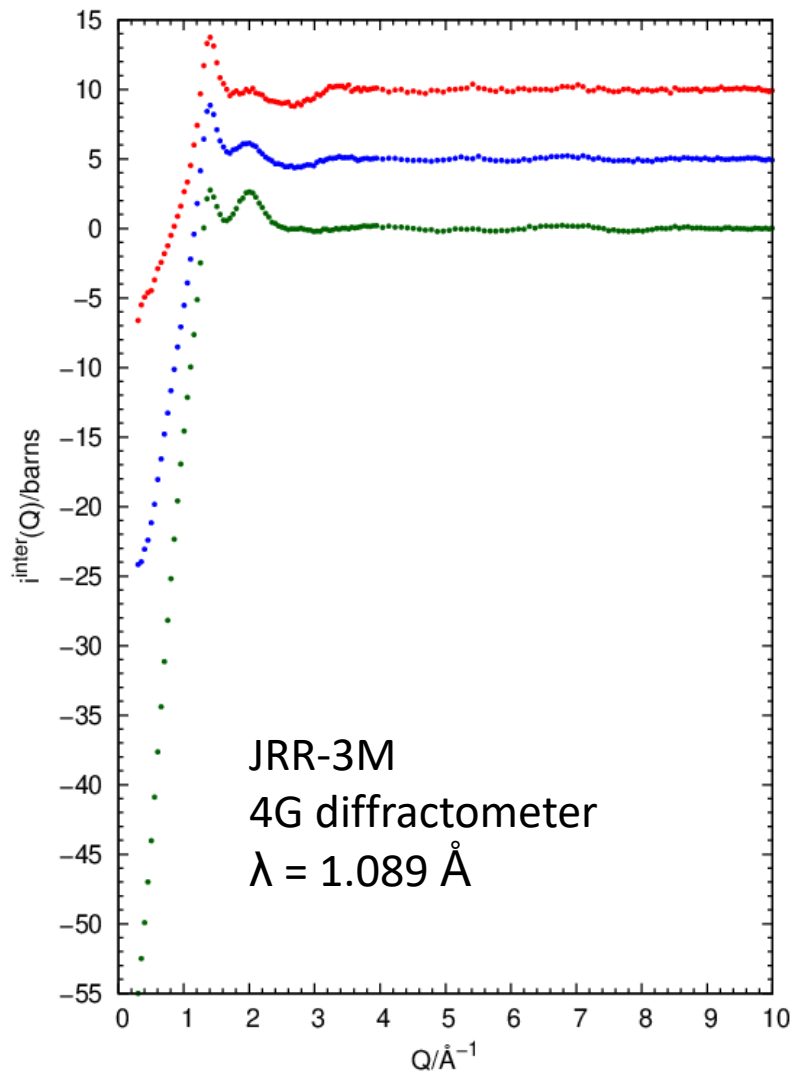
H:D = 32:68  
13h

H:D = 0.5:99.5  
7h



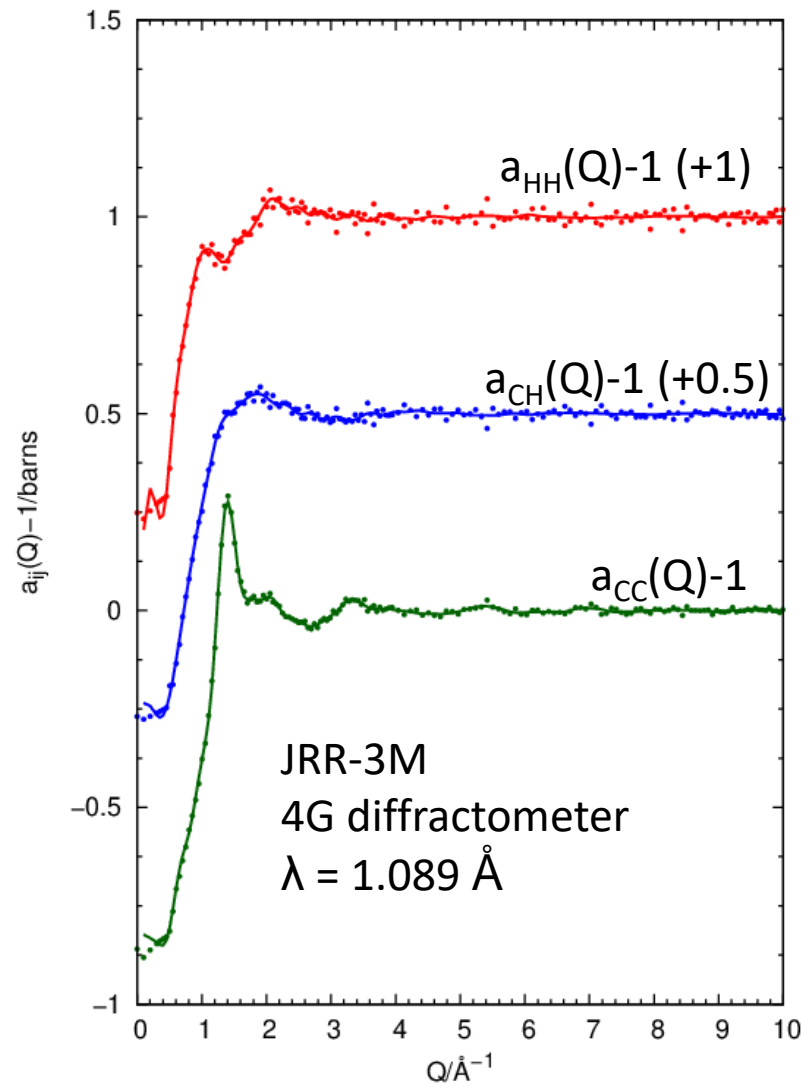
## Intermolecular interference terms

$C_6X_6$  (X: D,  $^0H$ ,  $^{02}H$ ) JRR-3M 4G spectrometer, 2021.10.11-13



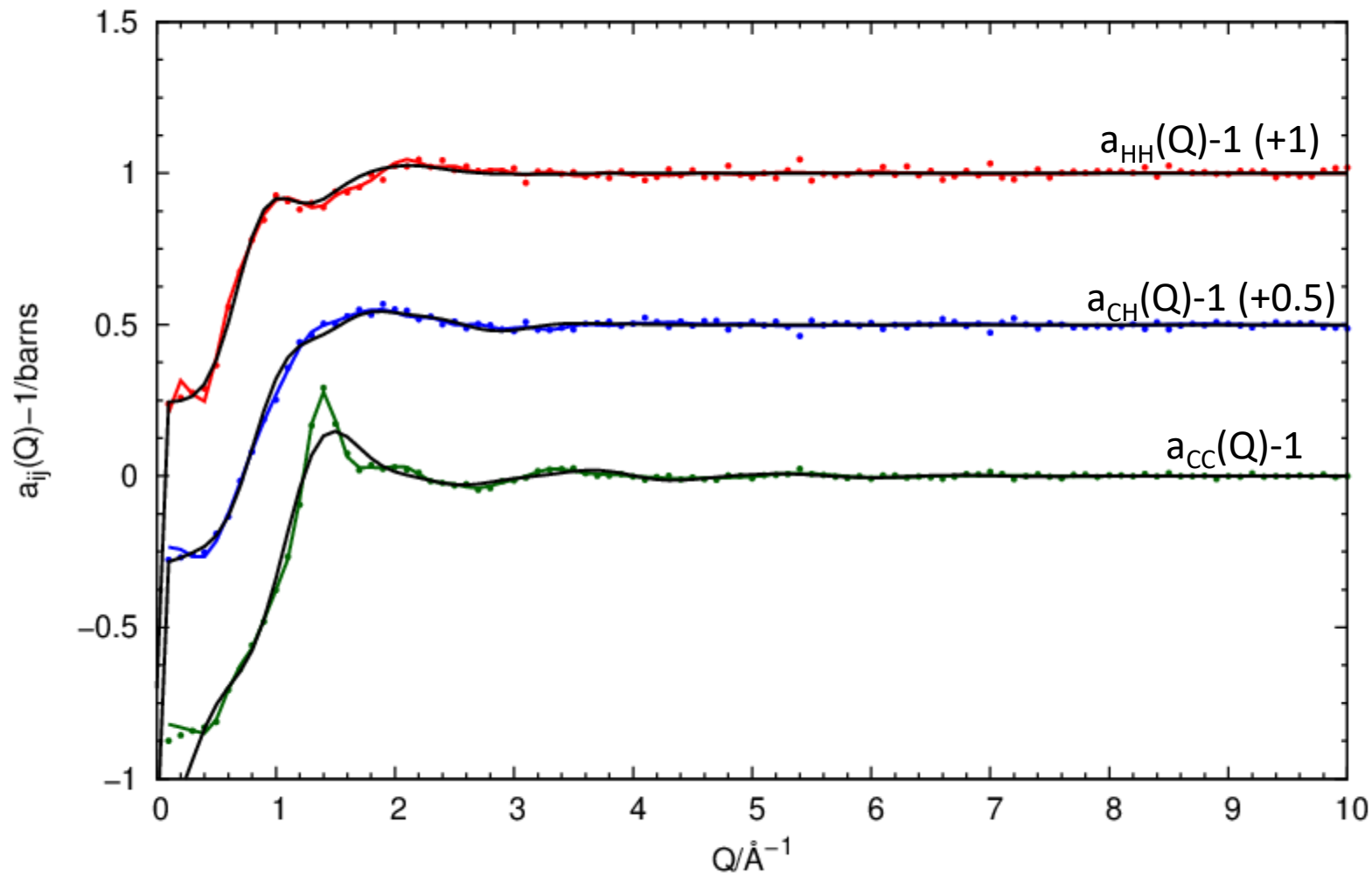
## Partial structure factors

$C_6X_6$  (X: D,  $^0H$ ,  $^{02}H$ ) JRR-3M 4G spectrometer, 2021.10.11-13



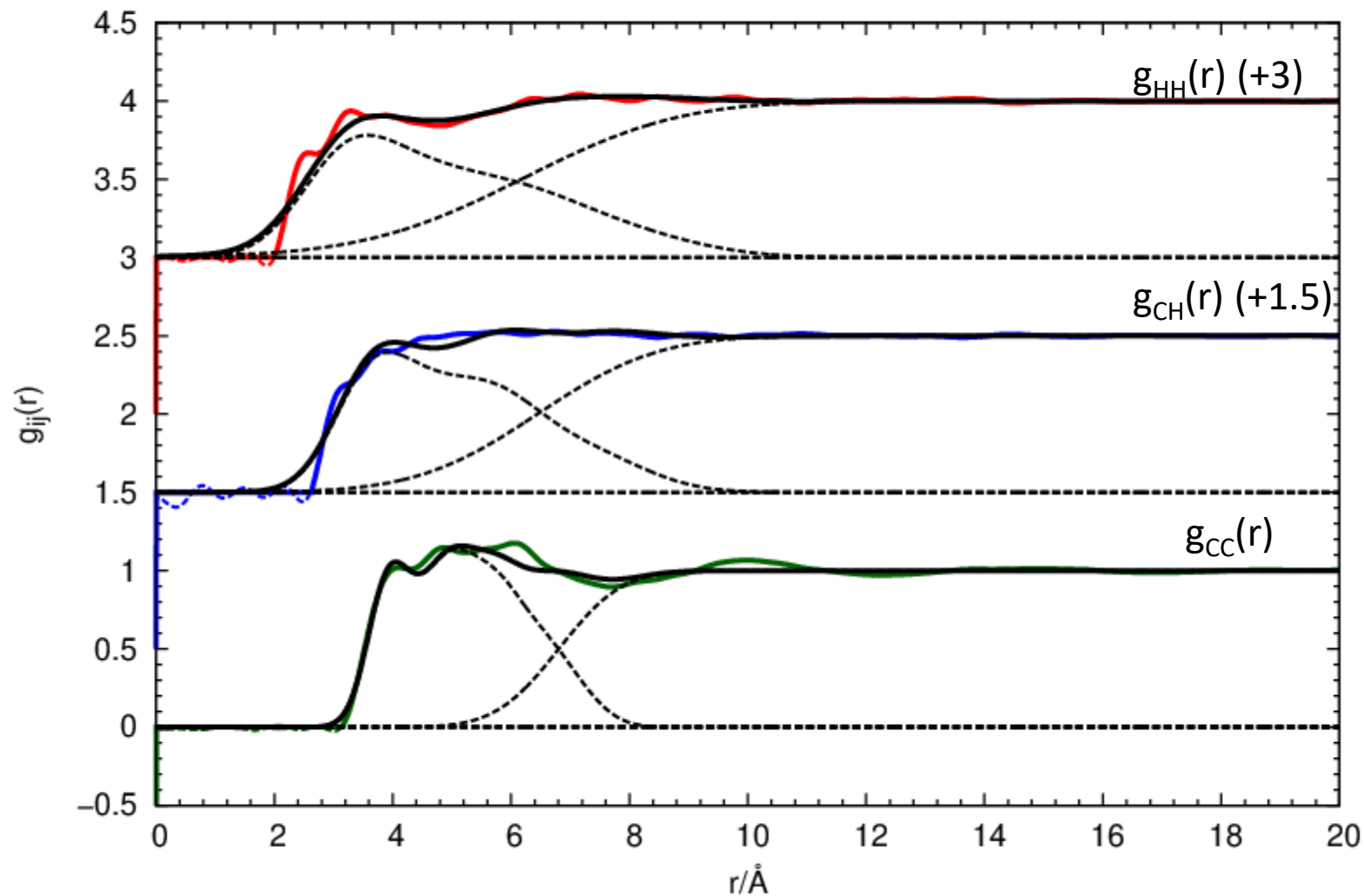
# Partial structure factors observed for liquid benzene

$C_6X_6$  (X: D,  $^0H$ ,  $^{02}H$ ) JRR-3M 4G spectrometer, 2021.10.11-13

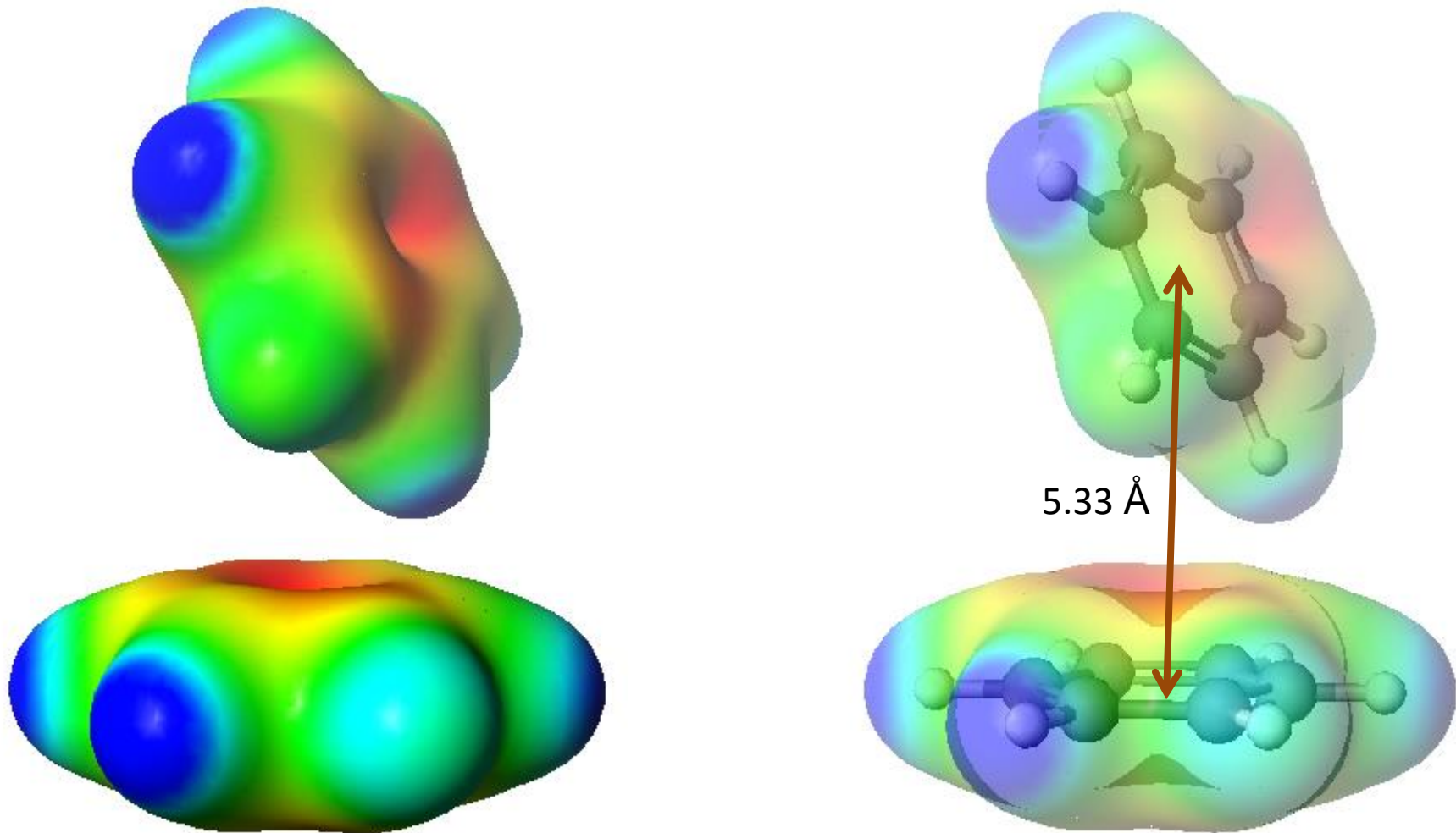


# Partial distribution functions observed for liquid benzene

$C_6X_6$  (X: D,  $^0H$ ,  $^{02}H$ ) JRR-3M 4G spectrometer, 2021.10.11-13

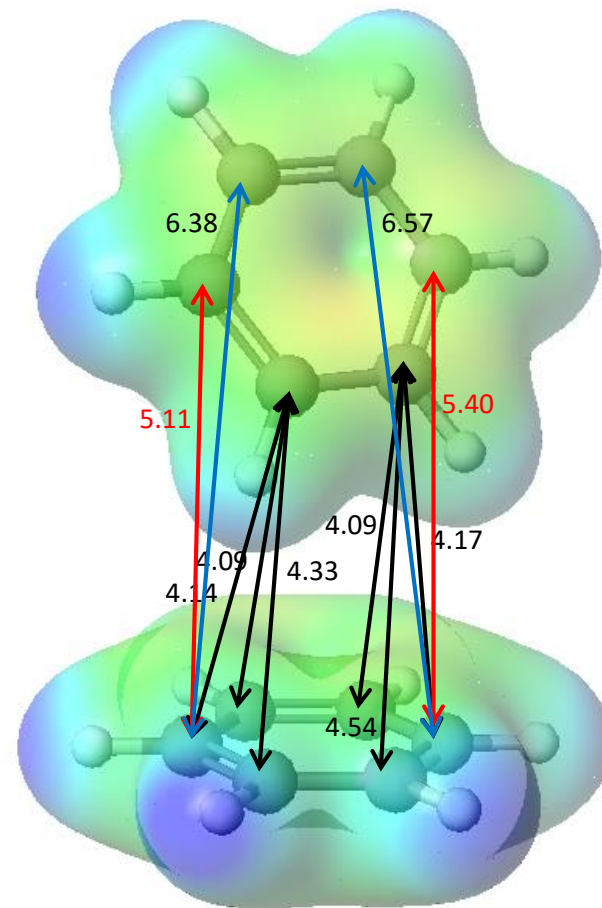
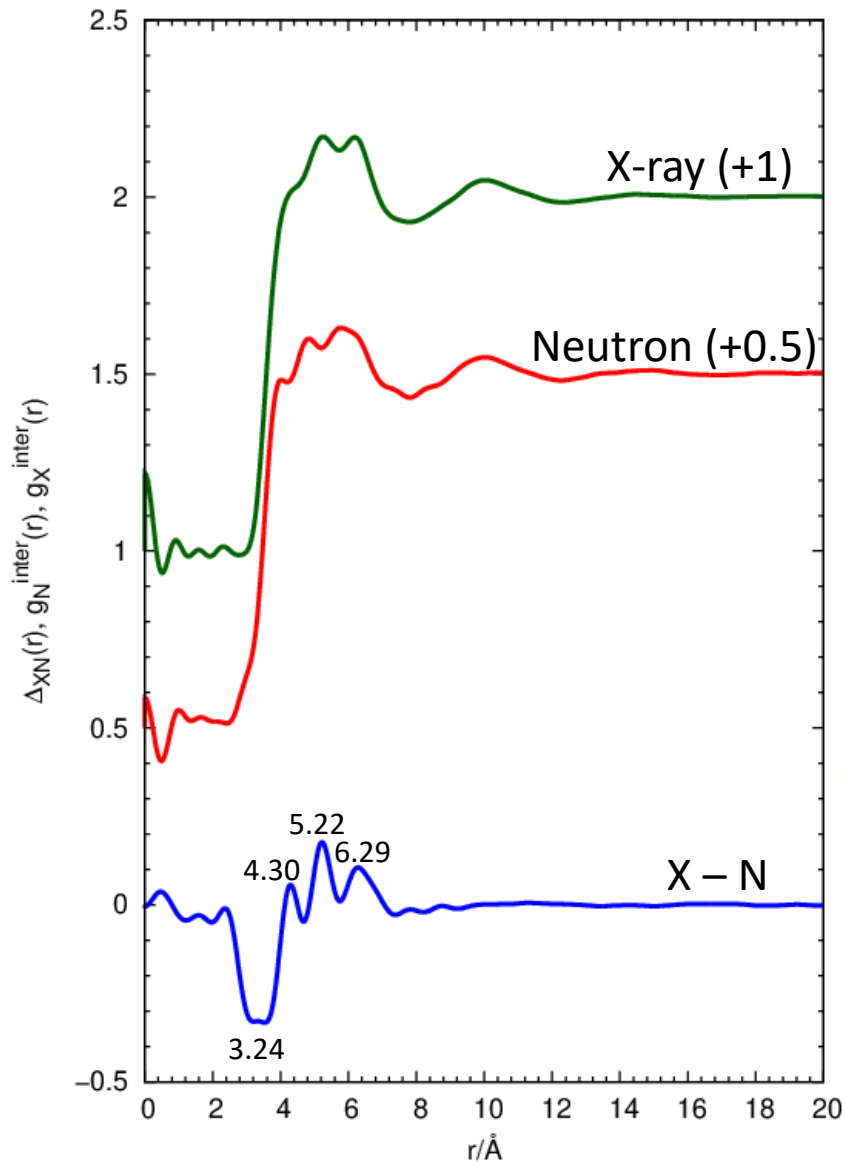


Orientational correlation between nearest neighbour benzene molecules  
Determined from neutron diffraction with H/D isotopic substitution  
method



# X-ray – neutron difference intermolecular difference distribution function

$C_6X_6$  (X: D,  $^0H$ ,  $^{02}H$ ) JRR-3M 4G spectrometer, 2021.10.11–13



DFT B88-LYP structure